Substitutions in a Flexible Loop of Horse Liver Alcohol Dehydrogenase Hinder the Conformational Change and Unmask Hydrogen Transfer[†,‡]

S. Ramaswamy,[§] Doo-Hong Park,[||,⊥] and Bryce V. Plapp*[,||]

Department of Molecular Biology, Swedish University of Agricultural Sciences, S-751 24 Uppsala, Sweden, and Department of Biochemistry, The University of Iowa, Iowa City, Iowa 52242

Received July 27, 1999; Revised Manuscript Received September 10, 1999

ABSTRACT: When horse liver alcohol dehydrogenase binds coenzyme, a rotation of about 10° brings the catalytic domain closer to the coenzyme binding domain and closes the active site cleft. The conformational change requires that a flexible loop containing residues 293−298 in the coenzyme binding domain rearranges so that the coenzyme and some amino acid residues from the catalytic domain can be accommodated. The change appears to control the rate of dissociation of the coenzyme and to be necessary for installation of the proton relay system. In this study, directed mutagenesis produced the activated Gly293Ala/Pro295Thr enzyme. X-ray crystallography shows that the conformations of both free and complexed forms of the mutated enzyme and wild-type apoenzyme are very similar. Binding of NAD^+ and 2,2,2-trifluoroethanol do not cause the conformational change, but the nicotinamide ribose moiety and alcohol are not in a fixed position. Although the Gly293Ala and Pro295Thr substitutions do not disturb the apoenzyme structure, molecular modeling shows that the new side chains cannot be accommodated in the closed native holoenzyme complex without steric alterations. The mutated enzyme may be active in the "open" conformation. The turnover numbers with ethanol and acetaldehyde increase 1.5- and 5.5-fold, respectively, and dissociation constants for coenzymes and other kinetic constants increase 40−2000-fold compared to those of the native enzyme. Substrate deuterium isotope effects on the steady state V or V/K_m parameters of 4−6 with ethanol or benzyl alcohol indicate that hydrogen transfer is a major rate-limiting step in catalysis. Steady state oxidation of benzyl alcohol is most rapid above a pK of about 9 for V and V/K_m and is 2-fold faster in D_2O than in H_2O. The results are consistent with hydride transfer from a ground state zinc alkoxide that forms a low-barrier hydrogen bond with the hydroxyl group of Ser48.

Horse liver alcohol dehydrogenase (ADH)[1] was one of the first enzymes for which the three-dimensional structures in two different conformational states, the free enzyme and an enzyme−coenzyme−substrate analogue complex, were described (*1*). Each subunit in the dimeric enzyme has two domains, a coenzyme binding domain with the Rossmann fold and a catalytic domain with the zinc ion to which substrates bind. When the ternary complex forms, the catalytic domain rotates about 10° so that the residues in the catalytic domain move closer to the coenzyme domain, and the cleft between domains closes (*2*). The closure requires that the loop with residues 293−298 from the coenzyme domain rearranges, providing space for some residues in the catalytic domain and some interactions with the coenzyme (Figure 1).

Structures of many complexes of ADH have been determined by X-ray crystallography. Most complexes with NAD^+, NADH, or a coenzyme and a good substrate analogue exhibit the closed conformation. In contrast, some complexes with coenzyme analogues or inhibitors and chemically modified enzymes remain in the open conformation (*4*). The conformational transition is associated with small changes in energetics (*2*), but it is not clear what interactions in the complexes are responsible for the change.

The kinetic mechanism is ordered bi-bi (*5*) with coenzyme binding first, and the isomerization of the enzyme−NAD^+ complex has been characterized by transient kinetics (*6*, *7*). Substrates apparently bind preferentially to the enzyme−coenzyme complex that has the closed conformation. During the conformational change, Ser48 and His51 from the catalytic domain form hydrogen bonds with the 2′- and 3′-hydroxyl groups of the nicotinamide ribose and set up the proton relay system that connects the water or substrate bound to the catalytic zinc with the bulk solvent (*8*). The substrate binding pocket also contracts. These changes seem to facilitate binding and reaction of the substrates, but it is not known if the conformational change is required for catalysis or if there are other intermediate states in the coenzyme binding reaction.

We studied the participation of residues in the loop with residues 293−298 by making substitutions of two residues

[†] This work was supported by NSF Grant MCB 95-06831 and NIH Grant AA00279 (B.V.P.) and the Swedish Agriculture and Forestry Research Foundation (S.R.).

[‡] The X-ray coordinates and structure factors for the apo and holo G293A/P295T enzymes have been deposited in the Protein Data Bank with entry names 1qlj and r1qljsf, and 1qlh and r1qlhsf, respectively.

* Corresponding author. E-mail: bv-plapp@uiowa.edu.

[§] Swedish University of Agricultural Sciences.

[||] The University of Iowa.

[⊥] Current address: Biologics Center, Mogam Biotechnology Research Institute, 341 Pojung-ri, Koosung-myon, Yongin-si, Kyonggi-do, Korea 449-910.

[1] Abbreviations: ADH, horse liver alcohol dehydrogenase; G293A/P295T, double substitution of Gly293 with Ala and Pro295 with Thr.

10.1021/bi991731i CCC: $18.00
Published on Web 09/30/1999

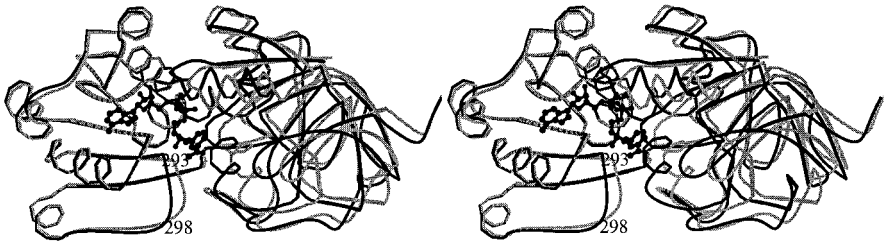

FIGURE 1: Comparison of the conformations of the native horse liver enzyme in the apo and holo forms. The apoenzyme is the open conformation shown as the gray line, and the holoenzyme is the closed ternary complex with NAD^+ and 2,3,4,5,6-pentafluorobenzyl alcohol (PDB entry 1hld) shown as the black line with the coenzyme in black. The α-carbons of the coenzyme binding domains (residues 176−292 and 299−314) on the left side of the structure were superimposed with O. The catalytic domains of the apo- and holoenzymes on the right side differ due to a relative rotation of about 10°. The flexible loop containing residues 293−298 also moves during the conformational change. The figure was prepared with MOLSCRIPT (*3*).

that could affect the flexibility of the loop and found one combination of mutations that produced an activated enzyme that does not change conformation as readily as the wild-type enzyme does, as shown by X-ray crystallography. Since the substitutions substantially decrease affinities for the coenzyme, hydrogen transfer could be studied with steady state kinetics.

EXPERIMENTAL PROCEDURES

Preparation of Enzyme. The phagemid pBPP/*Eq*ADH-E, which contains the cDNA for ADH under the control of the tac promoter, an ampicillin resistance gene, and the replication origin for f1 bacteriophage (*9*), was produced in *Escherichia coli* strain CJ236 as a single-stranded, uracil-containing DNA (antisense) by infection with helper phage VCMS13 from Stratagene. A partially random mutagenesis used degenerate oligodeoxyribonucleotide mutamers synthesized on an ABI394 synthesizer with the following sequences: GTC ATT GTG (A/C/T)(A/C/T)C GTA (A/G/T)(A/G/T)T CCT GAT TCC and C ATT GTG G(A/C/T)A GTA (A/G/T)CT CCT GAT, where the sites of mutation are underlined. These were phosphorylated on the 5′-ends and used in separate mutagenesis experiments along with a second primer, TGT TGA CAA TTA ATC ATC (*10*). After transformation in XL1-Blue cells (Stratagene) and selection for ampicillin-resistant colonies, plasmids were isolated and screened for the loss of an *Rsa*I restriction site (GTAC) that led to an increase in the fragment size from 436 to 491 bp. A total of eight different double mutations were introduced. The level of expression of ADH was determined in cells grown in 50 mL cultures of LB medium containing 100 μg/mL ampicillin and 12 μg/mL tetracycline and induced with 0.1 mM IPTG. Cells were lysed; the centrifuged homogenate was assayed for enzyme activity in a standard assay (*11*), and samples were subjected to gel electrophoresis on nondenaturing agarose gels at pH 8 where the enzyme migrates in the direction which is the opposite of those of almost all of the *E. coli* proteins (*12*). Good expression was obtained for the His293/Ser295, Asn/Ser, Thr/Asn, Glu/Thr, and Ala/Thr enzymes, whereas fair or poor expression was found for the Ile/Val, Leu/Ser, and Val/Thr enzymes. Of these enzymes, only the Ala293/Thr295 enzyme exhibited good activity, and indeed, this enzyme had much higher activity than the wild-type enzyme. The complete sequence of the mutated ADH cDNA was determined using the Sequenase kit from United States Biochemical to confirm the structure (*13*).

Enzyme for kinetic studies and crystallography was expressed, purified to homogeneity, and characterized by methods described previously (*9*). In addition, chromatography on a 7.5 mm × 30 cm Waters Protein Pak 300 SW column showed that the protein eluted at the same position as the enzyme isolated from horse liver by Boehringer Mannheim Biochemicals. Titration attempted with NAD^+ in the presence of 10 mM pyrazole failed to give an absorbing complex as found for the wild-type enzyme (*14*). In contrast, the active sites could be titrated with NADH in the presence of 100 mM isobutyramide (*15*).

Kinetic Studies. Steady state kinetic parameters were determined spectrophotometrically as described previously (*9*). The change in absorbance due to NADH was followed at 340 nm except when high concentrations of NADH required the use of 366 nm. Kinetic data were fitted with the appropriate programs (*16*). Standard errors for the fitted parameters were less than 25% of the values, which indicate that the values are well-determined (*16*), and usually between 5 and 20% of the values.

X-ray Crystallography. Crystals of the apoenzyme were produced by dialysis of 10 mg/mL enzyme against 4.5% 2-methyl-2,4-pentanediol in 50 mM tris(hydroxymethyl)-aminomethane-HCl at pH 8.4 and 5 °C. Crystals of the holoenzyme were produced by dialysis of 10 mg/mL enzyme against 12% 2-methyl-2,4-pentanediol in 50 mM ammonium *N*-[tris(hydroxymethyl)methyl]-2-aminoethanesulfonate buffer at pH 7.0 and 5 °C, with 1.3 mM NAD^+ and 400 mM 2,2,2-trifluoroethanol. The concentration of 2-methyl-2,4-pentanediol was raised finally to 25%. Crystals were flash-frozen, and data were collected at 100 K. Data for the apoenzyme were collected with an R-Axis II mounted on a rotating anode generator, and data for the holoenzyme were collected at the BW7B beamline at EMBL (DESY, Hamburg, Germany).

The data sets were processed using MOSFLM (*17*) and scaled using SCALA (*18*). The space group for the apoenzyme was very close to C-centered orthorhombic, but the $h + k =$ odd reflections were present, indicating the absence of centering. Although the crystals of the holo form diffract to 2.0 Å resolution, the data set is complete to only 2.5 Å resolution and is partial at higher resolution. The structure of the apo form of the enzyme was determined using AMORE (*19*) and the native refined apo liver alcohol dehydrogenase[2] as a model. The structure of the complexed form was determined by the same procedure using the refined apo form of the mutant enzyme. The structures were refined

with CNS (*20*) with rigid body refinement where the two domains were treated independently and with strict NCS symmetry for the apoenzyme assumed throughout. The distances for the ligands to the catalytic and structural zinc ions were fixed at the values found for other well-refined ADH structures. The maximum likelihood weighted $2F_o - F_c$ and $F_o - F_c$ maps were used to model the protein. O (*21*) was used for model building.

Model bias was avoided during the initial refinement of the mutated enzymes by retaining Gly293 and changing Pro295 to Ala. Moreover, the structures of the loops containing residues 291−299 and 364−366 were fitted into electron density omit maps calculated without those residues. As refinement progressed, density for the side chains of Ala293 and Thr295 became apparent and the mutated residues were included in further refinement.

During refinement of the holoenzyme, the NAD was not added to the model until the refinement converged at 2.5 Å resolution. At this stage, the $2F_o - F_c$ and the $F_o - F_c$ maps clearly showed density for the adenosine diphosphate part of the NAD but none for the nicotinamide ribose. The final few cycles of refinement used all of the data to 2.07 Å resolution, and the model was improved; however, no new water molecules were added.

The structures were checked using the server at the EMBL outstation at Hinxton and WHATIF (*22*) and Procheck (*23*). Both structures are well-refined. There are no outliers in the Ramachandran plot (except for Cys174, which is ligated to the catalytic zinc and has unusual angles in all ADH structures), and the scores in Procheck are better than for other structures refined at their respective resolutions.

RESULTS

Kinetic Characterization. The G293A/P295T substitutions produce an enzyme that has a specific activity that is higher than that of the wild-type enzyme isolated from horse liver. The turnover number of the mutant enzyme (with the protein concentration estimated from absorbance, $A_{280} = 0.455$ mg^{-1} cm^2) in the standard assay (*11*) at 30 °C is 14 s^{-1}, as compared to 2.3 s^{-1} for the wild-type enzyme, and 7.7 s^{-1} at 25 °C (1.8 s^{-1} for the wild-type enzyme). The physical properties of the mutated and wild-type enzymes are similar as they exhibit indistinguishable chromatographic and electrophoretic behavior. Titration with NADH in the presence of isobutyramide showed that all active sites of the mutant enzyme could bind NADH. The difference spectra also show that NADH bound to the enzyme has the absorption maximum of the reduced nicotinamide ring shifted from the 340 nm observed for free NADH to lower wavelengths such that the difference spectrum of free and enzyme-bound NADH exhibits a maximum at 347 nm ($\Delta\epsilon = 1.5$ mM^{-1} cm^{-1}) compared to a maximum at 355 nm ($\Delta\epsilon = 2.5$ mM^{-1} cm^{-1}) for the wild-type enzyme (*15*).

The kinetic constants for the G293A/P295T enzyme were determined from steady state initial velocity and product inhibition experiments. The results in Table 1 show that most kinetic constants for ethanol and acetaldehyde increase 2−3 orders of magnitude while turnover numbers increase 1.5−5.5-fold compared to the values for the wild-type enzyme. Similar effects are seen with benzyl alcohol. Since the dissociation constants for the coenzymes (K_{ia} and K_{iq}) increase, the mutations probably increase the rates of coenzyme dissociation, which are rate-limiting for turnover for the wild-type enzyme (*5*, *7*, *27*, *28*).

Table 1: Kinetic Constants for the Wild-Type E Isoenzyme and G293A/P295T Horse Liver Alcohol Dehydrogenases[a]

	E		G293A/P295T	
	CH_3CH_2OH CH_3CHO[b]	$C_6H_5CH_2OH$ C_6H_5CHO[c]	CH_3CH_2OH CH_3CHO[d]	$C_6H_5CH_2OH$ C_6H_5CHO
K_a (μM)	3.9	3.7	1900	2800
K_b (mM)	0.35	0.028	710	8.1
K_p (mM)	0.40	0.12	110	4.9
K_q (μM)	5.8	9.9	510	950
K_{ia} (μM)	27	120	1100	2000
K_{iq} (μM)	0.50	0.41	320	280
V_1 (s^{-1})	3.5	3.1	5.2	1.3
V_2 (s^{-1})	47	110	260	51

[a] Initial velocities were measured with varied concentrations of both substrates at 30 °C in 33 mM sodium phosphate buffer (pH 8.0) and 0.25 mM EDTA, unless stated otherwise. K_a, K_b, K_p, and K_q are the Michaelis constants for NAD^+, alcohol, aldehyde, and NADH, respectively. K_i values are inhibition constants, and V_1 and V_2 are the turnover numbers in the forward and reverse directions, respectively. [b] At 25 °C (*24*). [c] Studies at pH 7.0 and 30 °C (*25*). [d] At 25 °C.

Product and dead-end inhibition studies (Table 2) are generally consistent with an ordered bi-bi mechanism for benzyl alcohol, ethanol, and their respective aldehydes (*29*). In particular, 2,2,2-trifluoroethanol is an uncompetitive inhibitor against varied concentrations of NAD^+, and the aldehyde analogue, *N*-cyclohexylformamide (*30*), is uncompetitive against NADH, as expected for an ordered mechanism. On the other hand, 2,3,4,5,6-pentafluorobenzyl alcohol is a noncompetitive inhibitor against varied concentrations of ethanol, benzyl alcohol, or NAD^+, as indicated by systematic and significant changes in slope and intercept effects and variances that are at least 2-fold lower for noncompetitive inhibition than the variances for the fits to the equations for competitive or uncompetitive inhibition. The relative magnitudes of the slope and intercept inhibition constants indicate that pentafluorobenzyl alcohol binds most tightly to the enzyme−NAD^+ complex and more weakly to the free enzyme or other forms of the enzyme.

The inhibition constants for the dead-end inhibitors, which represent dissociation constants from the enzyme−coenzyme ternary complexes, are substantially increased for the mutated enzyme. For the wild-type enzyme, K_i for trifluoroethanol is 8.4 μM (*9*), whereas for the G293A/P295T enzyme, it is 4.1 mM (average of values in Table 2). The K_i for $C_6F_5CH_2OH$ is 3 μM for the wild-type enzyme (*31*) and 0.58 mM for the mutant enzyme. Likewise, the K_i for *N*-cyclohexylformamide is 8 μM for the wild-type enzyme (*30*) and 100 μM for the mutant enzyme, and the K_i for *N*-methylformamide is 1.4 mM (*32*) for the wild-type enzyme and 38 mM for the mutant enzyme. The increases in K_i values of 1 or 2 orders of magnitude (for formamides or fluoro alcohols, respectively) reflect significant changes in the binding environments.

The rate-limiting steps in the mechanism of oxidation of alcohols were probed with initial velocity studies of substrate

[2] The structure of the apoenzyme (*37*) was further refined with the data at 2.4 Å resolution to a final *R* value of 16.7% (T. A. Jones, S. Ramaswamy, and H. Eklund, unpublished results). The structure does not differ significantly from that deposited in the PDB with entry name 8adh, but only 175 water molecules were retained in the final structure.

Table 2: Product and Dead-End Inhibition Studies for G293A/P295T Liver Alcohol Dehydrogenase[a]

	substrate				
inhibitor	varied	fixed	pattern	K_{is} (mM)	K_{ii} (mM)
$C_6H_5CH_2OH$ (0−20)	C_6H_5CHO (1−5)	NADH (0.34)	noncomp	5.5	15
$C_6H_5CH_2OH$ (0−20)	NADH (0.067−0.33)	C_6H_5CHO (5)	noncomp	10	8.0
C_6H_5CHO (0−10)	$C_6H_5CH_2OH$ (3.3−20)	NAD^+ (9.5)	noncomp	6.0	16
CF_3CH_2OH (0−20)	CH_3CH_2OH (200−1000)	NAD^+ (10)	comp	3.8[b]	
CF_3CH_2OH (0−20)	NAD^+ (1−6)	CH_3CH_2OH (500)	uncomp		4.4[b]
N-methylformamide (0−300)	CH_3CHO (30−150)	NADH (0.2)	comp	38[b]	
N-cyclohexylformamide (0−1)	NADH (0.072−0.36)	CH_3CHO (75)	uncomp		0.10[b]
$C_6F_5CH_2OH$ (0−2)	CH_3CH_2OH (200−1000)	NAD^+ (10)	noncomp	0.56[b]	3.0
$C_6F_5CH_2OH$ (0−2)	$C_6H_5CH_2OH$ (3.3−20)	NAD^+ (10)	noncomp	0.60[b]	4.9
$C_6F_5CH_2OH$ (0−2)	NAD^+ (1−6)	CH_3CH_2OH (500)	noncomp	3.3	0.62[b]

[a] Initial velocities were measured at 30 °C in 33 mM sodium phosphate buffer (pH 8.0) and 0.25 mM EDTA. Concentrations (in millimolar) are listed in parentheses for each compound. Data were fitted to the equations for competitive (comp), noncompetitive (noncomp), and uncompetitive (uncomp) inhibition, where K_{is} is the slope inhibition constant and K_{ii} is the intercept inhibition constant (*28*). [b] K_i values were corrected for the concentration of fixed substrate, yielding the dissociation constants for binding of the inhibitors to the enzyme−coenzyme complexes.

Table 3: Substrate Isotope Effects for G293A/P295T Liver Alcohol Dehydrogenase with Various Alcohols[a]

substrate	K_a (μM)	K_b (mM)	K_{ia} (μM)	V_1 (s^{-1})	$^DV_1$	$^D(V_1/K_a)$	$^D(V_1/K_b)$
ethanol	3200	930	770	13	4.8	3.5	4.1
1-butanol	1400	18	1100	25	2.3	1.6	3.0
benzyl alcohol	2800	8.1	2000	1.3	5.9	5.5	5.9

[a] Initial velocities were measured at 30 °C in 33 mM sodium phosphate (pH 8.0) and 0.25 mM EDTA with varied concentrations of NAD^+ and alcohol. The deuterated alcohols included ethanol-d_5, 1-butanol-d_9, and benzyl alcohol-α,α-d_2. The superscript D represents the ratio of kinetic constants with protio and deuterio alcohols (*33*). Errors were propagated for calculation of isotope effects and were 7−10% of the values.

isotope effects (Table 3). The turnover numbers (V_1) differ for the three alcohols, indicating that dissociation of NADH is not a common rate-limiting step, as it is for the wild-type enzyme (*26*, *27*). Furthermore, the substantial isotope effects on V_1 indicate that hydrogen transfer is significantly rate-limiting, in contrast to the case for the wild-type enzyme, which has a $^DV_1$ of 1.1 for ethanol oxidation under the conditions used here (*12*). With ethanol and butanol as substrates, the isotope effects are consistent with a preferred ordered mechanism, in which hydrogen transfer and release of NADH are partially rate-limiting. The similar magnitudes of the isotope effects on the V and V/K_b parameters for benzyl alcohol oxidation suggest that the mechanism is random with hydrogen transfer being predominantly rate-limiting for turnover. Although the steady state results suggest that the mechanism is kinetically ordered, catalysis is limited by the chemical steps. The double mutation then permits investigation of the chemical characteristics of hydrogen transfer for oxidation of benzyl alcohol.

The pH dependence of the hydride transfer during benzyl alcohol oxidation was studied with steady state experiments (Figure 2). The results are described by a simple mechanism in which the unprotonated enzyme forms have maximal activity. The enzyme−NAD^+ complex has a pK of 9.3 (from the V_1/K_b parameter), perhaps due to the catalytic zinc water, and the enzyme−NAD^+−alcohol complex has a pK of 8.4 (from V_1), assigned to the alcohol bound to the zinc. This is in contrast to the activity of the wild-type enzyme on ethanol, which has a bell-shaped pH dependence of V_1/K_b with pK values of 6.7 and 9.0 and an almost pH-independent V_1 (*27*). The reaction of benzyl alcohol with the wild-type enzyme

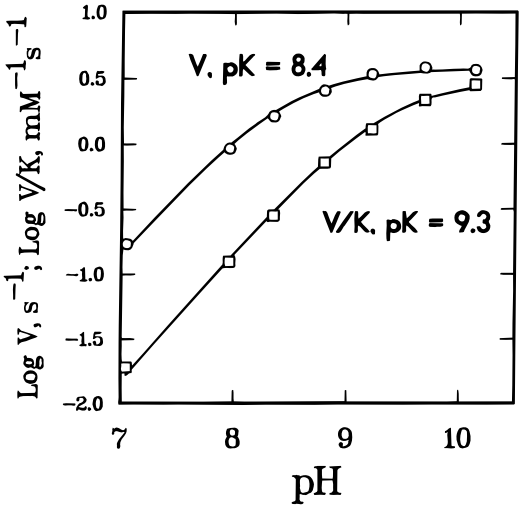

FIGURE 2: pH dependence of benzyl alcohol oxidation catalyzed by G293A/P295T ADH. The initial velocities for the steady state reaction were studied at 30 °C with 10 mM NAD^+ and varied concentrations of alcohol. The buffers contained 10 mM $Na_4P_2O_7$, 0.25 mM EDTA, and sufficient sodium phosphate buffer to adjust the pH and produce an ionic strength of 0.1 below pH 9.22, and 10 mM $Na_4P_2O_7$, 0.25 mM EDTA, and 10 mM sodium carbonate above pH 9.5 (*34*). At each pH, the data were fitted to the Michaelis−Menten equation, and the V_1 (○) and V_1/K_b (□) parameters were then fit to the logarithmic form of the equation $y_{obs} = y/(1 + [H^+]/K_1)$, which describes the mechanism where only unprotonated enzyme reacts with substrate: $HE^+ \rightleftharpoons E \rightarrow ES$. The fitted parameters gave pK_1 values of 8.41 ± 0.03 for the dependence of V_1 and 9.32 ± 0.04 for V_1/K_b, with limiting values at high pH of 3.7 ± 0.2 s^{-1} for V_1 and 3.1 ± 0.2 mM^{-1} s^{-1} for V_1/K_b.

was studied by transient methods, which showed that the maximum rate of oxidation occurs at a pH above a pK of 6.4 (*35*) with an H/D isotope effect (benzyl alcohol-α,α-d_2) of 3.6 (*7*). For the G293A/P295T enzyme, the substrate deuterium isotope effect on V_1 is 4.5 and on V_1/K_b is 4.9, independent of pH in the range from 7.0 to 9.7 (not shown).

The solvent isotope effect on the oxidation of protio- and deuteriobenzyl alcohols was studied so that the proton transfer and the transition state for hydride transfer could be characterized. For the wild-type enzyme, transient kinetics must be used for this study since dissociation of the enzyme−NADH complex limits turnover, but for the G293A/P295T enzyme, steady state kinetics can be used since hydride transfer is the major rate-limiting step. As shown in Table 4, the isotope effects for oxidation of protio as compared to

Table 4: Solvent and Substrate Isotope Effects for Oxidation of Benzyl Alcohol with Wild-Type and G293A/P295T Liver Alcohol Dehydrogenases[a]

enzyme	parameter	$^{D}H_2O$[b]	$^{D}D_2O$[c]	D_2O_h[d]	D_2O_d[e]
wild-type[f]	k	4.6	4.3	0.57	0.54
G293A/P295T[g]	V_1	4.5	4.0	0.51	0.46
	V_1/K_b	6.0	6.1	0.40	0.40

[a] Kinetic parameters were measured under conditions where the hydrogen transfer steps were rate-limiting and the pH was optimal. Benzyl alcohol-α,α-d_2 (MSD Isotopes) and 99.5% D_2O (Aldrich) were used. The buffers in H_2O and D_2O had the same ratio of buffering species for an equivalent pL (*36*). Buffers in D_2O were prepared from salts that were lyophilized from D_2O to exchange hydrogens. [b] Ratio of protio to deuterio benzyl alcohol in H_2O. [c] Ratio of protio to deuterio benzyl alcohol in D_2O. [d] Ratio of protio alcohol in H_2O to D_2O. [e] Ratio of deuterio alcohol in H_2O to D_2O. [f] From the exponential phase in transient kinetic experiments with 2 mM NAD^+ and 0.05−0.5 mM benzyl alcohol in 33 mM sodium phosphate buffer (pH 8.0) and 0.25 mM EDTA at 25 °C. A BioLogic SFM3 stopped-flow instrument with a dead time of 2.5 ms was used, with detection of NADH production by absorbance at 331 nm. The first-order rate constants for the "burst" phase were extrapolated to infinite concentration by fitting to the Michaelis−Menten equation, giving a value of 24 s^{-1} with benzyl alcohol in H_2O buffers. [g] From steady state kinetic experiments with 10 mM NAD^+ and 0.96−8 mM benzyl alcohol in 10 mM $Na_4P_2O_7$ and 10 mM sodium carbonate buffer (pH 10) and 0.25 mM EDTA at 30 °C. Data were fitted to the Michaelis−Menten equation; for benzyl alcohol oxidation in H_2O, V_1 was 3.4 s^{-1} and V_1/K_b was 2.1 mM^{-1} s^{-1}.

deuterio substrates range from 4 to 6 for wild-type and G293A/P295T enzymes acting in H_2O or D_2O. Significantly, the reactions are faster in D_2O, described by inverse solvent isotope effects of 0.40−0.57, and the substrate and solvent isotope effects are independent of one another. The isotope effects indicate that hydride transfer is accompanied by proton movements during the oxidation of benzyl alcohol.

X-ray Crystallography. The substantial changes in kinetic characteristics caused by the G293A/P295T substitutions suggested that the structure of the enzyme or its complexes might be altered. Thus, we crystallized the mutated enzyme under the conditions used previously for the apoenzyme (*37*) or for the holoenzyme (*38*) but with NAD^+ and 2,2,2-trifluoroethanol. The data collection and refinement statistics are summarized in Table 5.

The three-dimensional structures of both forms of the enzyme are very similar to one another and essentially can be superimposed on the wild-type apoenzyme structure described originally (*37*). Thus, the cleft between the coenzyme and catalytic domains is "open" rather than closed as found for ternary complexes (*38*). The rms deviations for superpositioning the coenzyme binding domains (residues 176−292 and 299−314) of the apo and holo forms of the wild-type and G293A/P295T enzymes are less than 0.3 Å, comparable to the values found for other ADH structures. The complete molecules of the apo and holo forms of the G293A/P295T enzyme could be superpositioned onto the native apoenzyme with rms deviations of 0.37 and 0.45 Å, respectively. There are some minor differences in the structures, perhaps due to the crystal packing, as the space groups are different. The apoenzyme form of the G293A/P295T enzyme has the whole dimeric molecule as the asymmetric unit, in contrast to the wild-type apoenzyme, which has one subunit in the asymmetric unit. The structures of the subunits of the G293A/P295T apoenzyme are not significantly different from one another, and strict noncrystallographic symmetry was applied during refinement. The complexed form of the G293A/P295T enzyme has one subunit in the asymmetric unit, whereas most other holoenzyme complexes have one or two molecules in the asymmetric unit.

Table 5: X-ray Data and Refinement Statistics for Horse Liver Alcohol Dehydrogenase G293A/P295T in the Apo and Holo Forms

	apo[a]	holo[b]
space group	$P2_12_12_1$	$C222_1$
cell dimensions (Å)	55.1, 72.9, 180.2	55.1, 73.7, 180.5
no. of subunits per asymmetric unit	2	1
resolution range (Å)	20.0−2.8	20.0−2.1
no. of reflections (unique, total)	17446, 49060	18016, 44823
completeness (%) (outer shell)	94.2 (87.8)	79.2 (57.4)
R_{sym} (%) (outer shell)[c]	10.2 (22.1)	11.2 (30.1)
mean $\langle I\rangle/\sigma\langle I\rangle$ (outer shell)	5.9 (3.2)	4.8 (2.4)
R_{value}, R_{free}, test %[d]	22.6, 25.7, 4.8	20.9, 25.4, 4.1
rsmd for bond distances[e]	0.010	0.010
rmsd for bond angles	1.3	1.3
no. of water molecules per subunit	88	88

[a] Free enzyme at pH 8.4. [b] Complex crystallized with NAD^+ and trifluoroethanol at pH 7. [c] $R_{sym} = (\Sigma|I - \langle I\rangle|)/\Sigma\langle I\rangle$, where I is the integrated intensity of a given reflection. [d] $R_{value} = (\Sigma||F_o| - k|F_c||)/\Sigma|F_o|$, where k is a scale factor. The R_{free} values were calculated with the indicated percentage of reflections not used in the refinement. [e] Root-mean-square deviations (rmsd) from ideal geometry of the final model.

A critical test for the crystallography was the confirmation of the substitutions of the amino acid residues. The structures of both the apoenzyme and complexed forms were refined with residues Gly293 and Ala295 in the model until the electron density maps clearly indicated that the substitutions were present. Figure 3 shows the final maps with the data to 2.1 Å resolution and the loop region in the complexed G293A/P295T enzyme, along with two water molecules, which were not located in the wild-type apoenzyme structure refined at 2.4 Å resolution. One of these waters forms hydrogen bonds with backbone atoms of residues 292 and 293 and a carboxylate oxygen of Glu267, which is buried in the structure. There is room for a water in the wild-type apoenzyme structure. The other water interacts with the carbonyl O of Gly270 and the amide N and hydroxyl group of Thr295. (The hydroxyl group of Thr295 also interacts with the carboxylate of Asp297.) This water would be displaced by the side chains of Pro295 and Ser298 in the wild-type structure. However, in the G293A/P295T enzyme, the positions of Ser298 and Asp297 are somewhat uncertain, as indicated by high temperature factors (more than 40 for residues 295−299). The G293A substitution is readily accommodated in the structure of the wild-type apoenzyme, since the extra methyl group extends into the open cleft. On the other hand, the P295T substitution allows some new hydrogen bonding interactions and appears to allow some flexibility in the loop.

Although the G293A/P295T enzyme that was crystallized in the presence of NAD^+ and trifluoroethanol has the open conformation of the wild-type apoenzyme, coenzyme is bound, as demonstrated in Figure 4. The positioning of the adenosine and pyrophosphate moieties is clear, but the nicotinamide riboside is not firmly fixed, as no good density was observed. Several positions were tried; however, the modeling was not confirmed by further refinement, and the nicotinamide riboside is arbitrarily positioned approximately

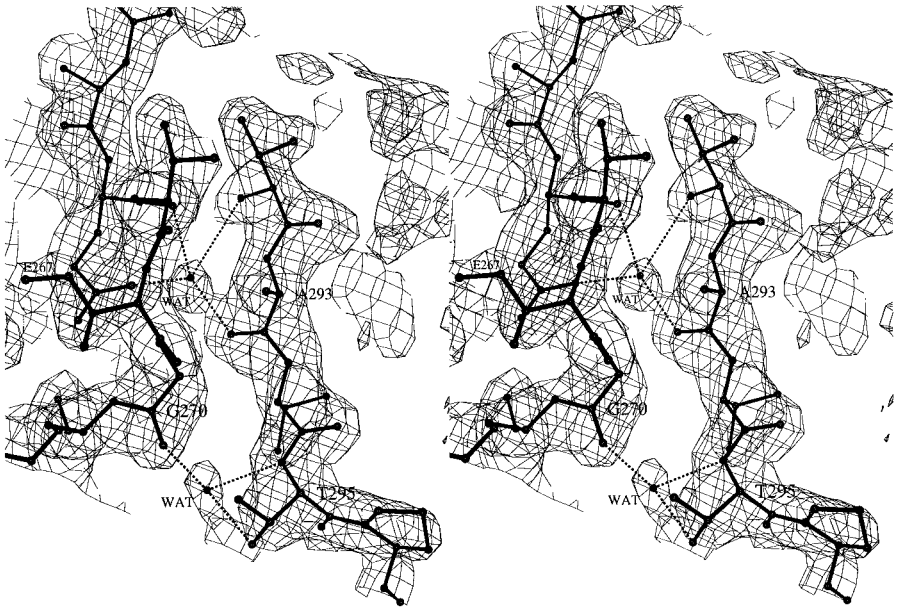

FIGURE 3: Structure of the flexible loop in G293A/P295T ADH. The final $2F_o - F_c$ electron density map for residues 292−295 and 267−270 and bound waters is shown, with all data to 2.07 Å resolution for the holoenzyme.

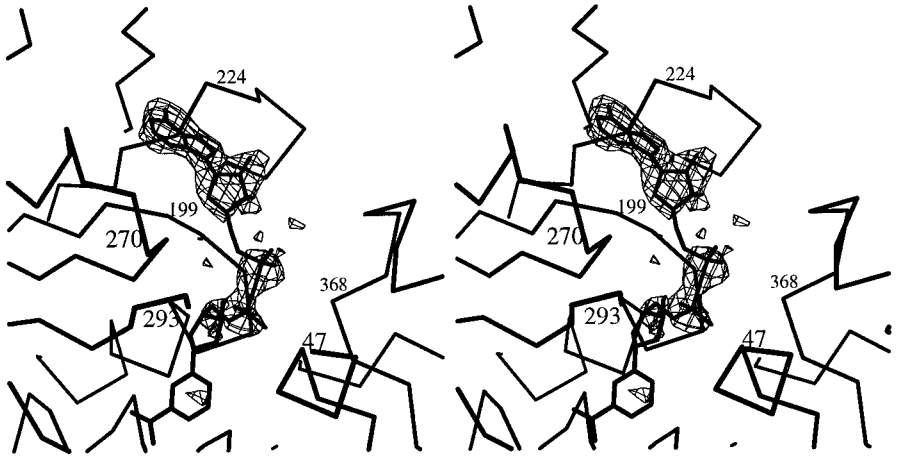

FIGURE 4: Location of the adenosine diphosphate moiety in the coenzyme binding domain of G293A/P295T ADH crystallized in the presence of NAD^+ and trifluoroethanol. The $F_o - F_c$ electron density map was calculated without including the coordinates for the coenzyme.

as it is found in the wild-type holoenzyme. Moreover, no good density was observed for trifluoroethanol bound to the catalytic zinc. Instead, the zinc has a water molecule making up the fourth ligand, as is found in the native apoenzyme (*37*).

We do not know why the nicotinamide riboside and trifluoroethanol are not visible in the structure. The concentrations of NAD^+ and trifluoroethanol used for the crystallization should have converted more than 95% of the enzyme into the ternary complex, as calculated from the dissociation constants listed in Tables 1 and 2. The 2-methyl-2,4-pentanediol precipitant (25% final concentration) could compete with the binding of trifluoroethanol, but no density for the diol is observed. The wild-type enzyme crystallized with either NAD^+ or NADH has the closed conformation, and some electron density that can be attributed to the diol is near the zinc (*39*). It appears that the inability of the enzyme to change conformation allows the nicotinamide riboside to move around in a variety of positions and that an optimal site for binding of alcohol is not formed. The spectral change at 347 nm when NADH binds to the enzyme in the presence of isobutryamide suggests that the environment of the reduced nicotinamide ring in the mutated enzyme is somewhat different than in the native enzyme.

DISCUSSION

The conformation of horse liver alcohol dehydrogenase usually changes when coenzyme and a substrate or substrate analogue bind (*40*). The change requires that the loop with residues 293−298 of the coenzyme binding domain rearranges so that the catalytic domain can move to close the active site cleft. Enzyme complexed with NAD^+ or NADH, some coenzyme analogues, or NAD(H) and a good substrate analogue crystallize in the closed form, whereas enzyme bound to coenzyme analogues with substituted nicotinamide rings often does not (*4*, *41*). Moreover, chemically modified enzymes [carboxymethyl-Cys46 (*42*) or isonicotinimidyl-Lys228 (*43*)] remain in the open form even in the presence of the coenzyme. The study presented here demonstrates that mutations in the flexible loop can hinder the conformational change and also substantially affect kinetic parameters for catalysis, making hydrogen transfer in the central complexes a major rate-limiting step in catalysis.

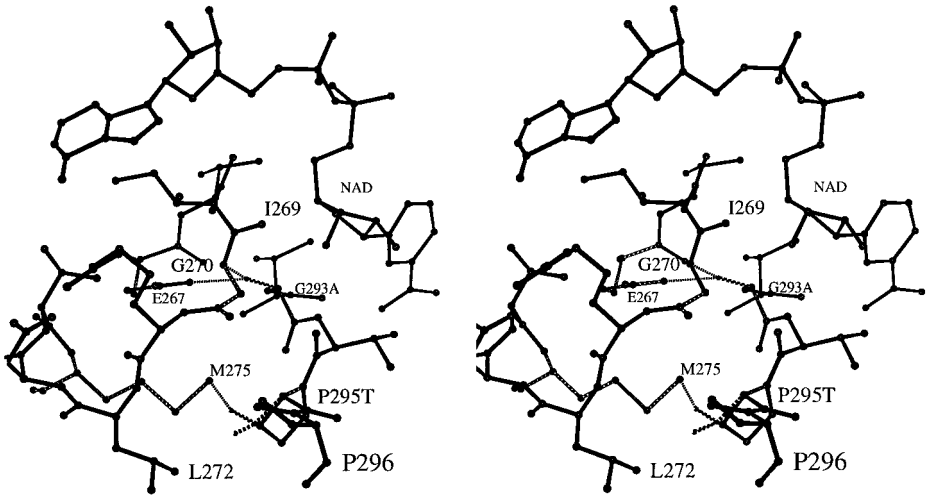

FIGURE 5: Potential steric hindrance due to G293A/P295T substitutions in a holoenzyme model. The structure of the ternary complex with NAD^+ and pentafluorobenzyl alcohol (PDB entry 1hld) was "mutated" with O. The mutated residues are represented by the dashed lines, superimposed on the solid lines of the native structure. The steric conflicts between the methyl group of Ala293 and the amide N of Gly270 or the carboxylate of Glu267 and the conflict between the hydroxyl group of Thr295 and the ϵ-methyl group of Met275 are represented by the dotted lines. The close contacts are 2.6−2.9 Å long and could not be accommodated in the structure without changes in the peptide backbone.

Structural Results. The G293A/P295T enzyme, with or without bound coenzyme, has a conformation that is the same, within the limits of resolution, as the "open" form of the wild-type apoenzyme. There are a few differences at residues 1−3, 298, and 364−366, but these are regions with high temperature factors. In contrast, the conformation of the wild-type holoenzyme, e.g., complexed with NADH and dimethyl sulfoxide or NAD^+ and 2,3,4,5,6-pentafluorobenzyl alcohol, is closed and has a different position for the loop with residues 293−298 (*31*, *38*).

Figure 3 shows that the mutations can be accommodated in the structure of the wild-type apoenzyme and that the P295T substitution permits an interaction with a water molecule that coincides with the movement of Ser298. Molecular modeling, however, suggests that the two substitutions could not be accommodated in the wild-type holoenzyme structure without causing some structural changes. Figure 5 shows that there would be steric conflicts in the closed form of the wild-type holoenzyme. These might be relieved by some rearrangements if the enzyme were to change conformation, but the conflicts suggest that the substitutions are energetically unfavorable for the closed conformation.

Sequence alignments of more than 100 members of the extended alcohol dehydrogenase family (*44*, *45*) show that Gly293 is almost completely conserved, with Asn replacing the Gly in four microbial enzymes, including two for which three-dimensional structures have been determined (*46*). The conformation of the loop in the tetrameric holoenzymes from *Clostridium beijerinckii* and *Thermoanaerobacter brockii* (PDB entries 1kev and 1ykf) is similar to that found in the wild-type horse holoenzyme, but small structural differences accommodate Asn266.

Pro295 is replaced by a great variety of residues in the alcohol dehydrogenase family. The corresponding residues in the holoenzymes from *C. beijerinckii* and *T. brockii*, His268 and Phe268, respectively, are accommodated in a slightly displaced loop. Cod ADH (PDB entry 1cdo) differs from the horse enzyme in residues 294−298, and the loops in the dimeric holoenzyme have a very different conformation than those found in the horse enzyme. Interestingly, the closure of the domains in the cod enzyme is different in the two subunits, with one similar to that of the wild-type horse apoenzyme and the other similar to that of the holoenzyme (*47*). Crystal packing interactions may account for the asymmetry.

The G293A/P295T enzyme is catalytically active, with turnover numbers increased as compared to those for the wild-type enzyme, although catalytic efficiency, as expressed as V_1/K_b or V_1/K_bK_{ia}, is considerably decreased. The activity means that the enzyme must be able to form the complex with NAD^+ and alcohol, but it is not clear if the active complex has the closed conformation. The structure of the holoenzyme shows that NAD binds, but the nicotinamide ring, the nicotinamide ribose, and the trifluoroethanol are not visible in the electron density maps. Thus, the structure of the holoenzyme does not provide a picture of the active ternary complex. The active complex most likely has the alcohol ligated to the catalytic zinc, and modeling suggests that the nicotinamide ring could fit into a position that is suitable for direct hydrogen transfer. The structure of the G293A/P295T enzyme might rearrange to relieve the steric conflicts shown in Figure 5 and bind coenzyme and substrate in a closed conformation. However, this would occur less readily than with the wild-type enzyme, and the active complex of the mutated enzyme might only form transiently at a low steady state concentration. We suggest, however, that the structural and kinetic studies indicate that the active ternary complex has an open conformation.

Hydrogen Transfer Mechanism. The altered pH dependence of the G293A/P295T enzyme suggests that the proton relay system that includes His51 is not installed in the enzyme−NAD^+ or enzyme−NAD^+−alcohol complexes. Figure 6 shows the structural differences between wild-type apo- and holoenzymes and illustrates that the conformational change is required to bring His51 close to the nicotinamide ribose. The p*K* values of 7.6 and 6.4 for the enzyme−NAD^+ or enzyme−NAD^+−alcohol complexes for native enzyme

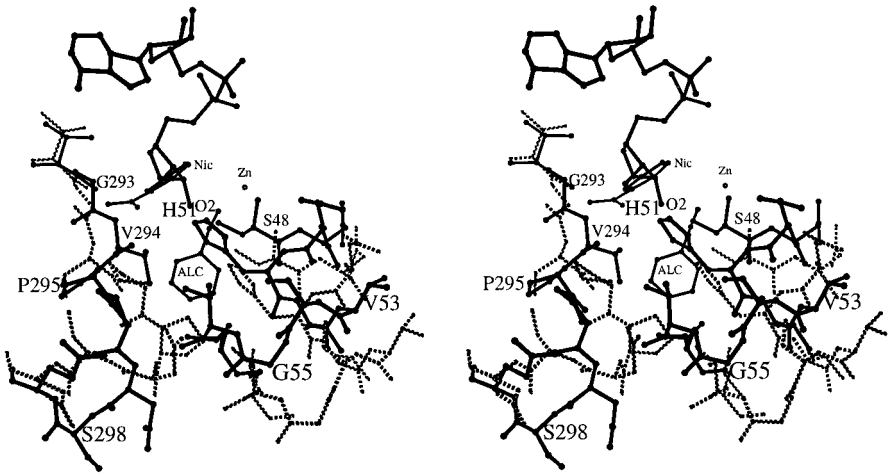

FIGURE 6: Comparison of the active site region of native apo- and holoenzymes. The coenzyme binding domains of the apoenzyme (in dashed lines, PDB entry 8adh) and the holoenzyme ternary complex (in solid lines, PDB entry 1hld) were superimposed with O, and the conformational changes in the flexible loop and the helix including His51 are shown.

Scheme 1

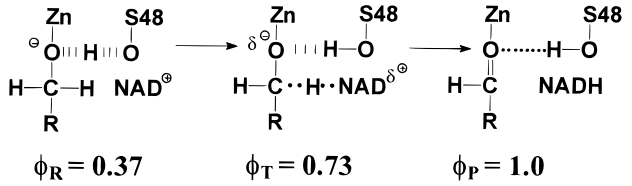

(*48*) are shifted substantially, to values of 9.3 and 8.4, respectively, for the double mutant enzyme. The p*K* of 9.3 could correspond to the zinc-bound water in the enzyme−NAD^+ complex and the p*K* of 8.4 to the zinc-bound alcohol in the enzyme−NAD^+−alcohol complex. If His51 formed a hydrogen bond to the 2′-hydroxyl of the nicotinamide ribose, as in the ternary complexes of the holoenzyme (*31*), the p*K* values should be decreased due to the facilitation of proton release.

The solvent and substrate isotope effects are independent of one another (Table 4) as is expected for concerted reactions, where the proton and hydride are transferred simultaneously rather than stepwise (*49*). We suggest that the isotope effects for the reaction in the ternary complex of alcohol dehydrogenase (k or V_1 in Table 4) are described by a mechanism in which the zinc-bound alkoxide makes a low-barrier hydrogen bond with the hydroxyl group of Ser48 in the reactant state, and the charge on the alkoxide diminishes in the transition state as the aldehyde forms, as shown in Scheme 1. In this mechanism, the environment of the hydrogen-bonded proton changes synchronously with the transfer of the hydride ion from the alcohol to the NAD^+. Scheme 1 is based on proton inventory data for the transient oxidation of ethanol by wild-type horse liver alcohol dehydrogenase, which are described by fractionation factors of 0.37 for the reactant state alkoxide and 0.73 for the transition state (*7*) and have an overall isotope effect ($k_{HOH}/k_{DOD} = \phi_R/\phi_T$) of 0.5.

The fractionation factors are consistent with established values for the hydrogen of a hydroxyl group binding to an alkoxide ion in a hydrophobic environment, with ϕ values of 0.27−0.47, and a fractionation factor for a hydrogen bond with a neutral species of about 1.0 (*50*). Alcohol dehydrogenase facilitates catalysis by stabilizing the intermediate alkoxide, which should undergo faster hydrogen transfer than would zinc-bound alcohol. In contrast to the role proposed for low-barrier hydrogen bonds in stabilizing transition states (*51*), ADH facilitates formation of a reactant state. The faster rate of hydride transfer in D_2O is consistent with a study of the gas phase reaction of microhydrated fluoride with methyl chloride, which indicates that the faster rate with D_2O than with H_2O arises because protium interacts more tightly than deuterium with the fluoride and leaves less energy for crossing the activation barrier (*52*).

Since both the wild-type and mutated enzymes exhibit similar inverse solvent isotope effects, it appears that the interaction of the zinc-bound alcohol oxygen with the hydroxyl group of Ser48 is responsible for the low fractionation factors and that His51 is not required. In the structure of the native enzyme complexed with NAD^+ and 2,3,4,5,6-pentafluorobenzyl alcohol (*31*), extended to a resolution of 1.25 Å (unpublished results), the distance between the two oxygens is 2.5 Å, consistent with a low-barrier hydrogen bond. The solvent isotope effects on V_1/K_b (Table 4) may be explained with a mechanism in which the reactant state enzyme−NAD^+ complex with the zinc-bound hydroxide, with a fractionation factor of 0.29, binds alcohol and leads to the transition state with a fractionation factor of 0.73 ($\phi_R/\phi_T = 0.4$). In the structure of the refined apoenzyme, the distance between the oxygens of the zinc-bound water and the hydroxyl group of Ser48 is short, at 2.5 Å, but the value is not certain as the resolution of the data is 2.4 Å.

The substitutions in the flexible loop of liver alcohol dehydrogenase show that the conformational change may be hindered by small structural changes. The changes significantly decrease the affinity for coenzymes and substrate analogues and make hydrogen transfer rate-limiting under steady state conditions. The mutated enzyme may be active in an open conformational state, which does not have His51 installed in the hydrogen-bonded system. His51 apparently facilitates deprotonation of the zinc-bound water in the wild-type enzyme (*53*), and the pH dependencies for the ionization of the zinc-bound ligands, water or alcohol, are increased by about 2 pH units due to the substitutions in the loop. Inverse solvent isotope effects lead to the conclusion that the zinc-bound alkoxide makes a strong hydrogen bond with

the hydroxyl group of Ser48 and is thus activated for hydride transfer.

ACKNOWLEDGMENT

We thank Kristine B. Berst for purification of the enzyme for crystallography and Fusheng Tang for doing the inhibition experiments with the formamides.

REFERENCES

1. Eklund, H., and Brändén, C.-I. (1979) *J. Biol. Chem. 254*, 3458−3461.
2. Colonna-Cesari, F., Perahia, D., Karplus, M., Eklund, H., Brändén, C.-I., and Tapia, O. (1986) *J. Biol. Chem. 261*, 15273−15280.
3. Kraulis, P. (1991) *J. Appl. Crystallogr. 24*, 946−950.
4. Eklund, H., and Brändén, C.-I. (1987) in *Biological Macromolecules and Assemblies: Volume 3-Active Sites of Enzymes* (Jurnak, F. A., and McPherson, A., Eds.) pp 73−141, Wiley, New York.
5. Wratten, C. C., and Cleland, W. W. (1963) *Biochemistry 2*, 935−941.
6. Sekhar, V. C., and Plapp, B. V. (1988) *Biochemistry 27*, 5082−5088.
7. Sekhar, V. C., and Plapp, B. V. (1990) *Biochemistry 29*, 4289−4295.
8. Eklund, H., Plapp, B. V., Samama, J.-P., and Brändén, C.-I. (1982) *J. Biol. Chem. 257*, 14349−14358.
9. Park, D.-H., and Plapp, B. V. (1991) *J. Biol. Chem. 266*, 13296−13302.
10. Kunkel, T. A., Roberts, J. D., and Zakour, R. A. (1987) *Methods Enzymol. 154*, 367−382.
11. Plapp, B. V. (1970) *J. Biol. Chem. 245*, 1727−1735.
12. Park, D.-H., and Plapp, B. V. (1992) *J. Biol. Chem. 267*, 5527−5533.
13. Sanger, F., Nicklen, S., and Coulson, A. R. (1977) *Proc. Natl. Acad. Sci. U.S.A. 74*, 5463−5467.
14. Theorell, H., and Yonetani, T. (1963) *Biochem. Z. 338*, 537−553.
15. Theorell, H., and Yonetani, T. (1964) *Arch. Biochem. Biophys. 106*, 252−258.
16. Cleland, W. W. (1979) *Methods Enzymol. 63*, 103−138.
17. Leslie, A. G. W. (1992) in *Joint CCP4 and ESF-EACMB Newsletter on Protein Crystallography No. 26*, Daresbury Laboratory, Warrington, U.K.
18. CCP4 Suite (1994) *Acta Crystallogr. D50*, 760−763.
19. Navaza, J. (1994) *Acta Crystallogr. 50*, 157−163.
20. Brünger, A. T., Adams, P. D., Clore, G. M., DeLano, W. L., Gros, P., Grosse-Kunstlev, R. W., Jiang, J. S., Kuszewski, J., Nilges, M., Pannu, N. S., Read, R. J., Rice, L. M., Simonson, T., and Warren, G. L. (1998) *Acta Crystallogr. D54*, 905−921.
21. Jones, T. A., Zou, J. Y., Cowan, S. W., and Kjeldgaard, M. (1991) *Acta Crystallogr. A47*, 110−119.
22. Vriend, G. (1990) *J. Mol. Graphics 8*, 52−56.
23. Laskowski, R. A., MacArthur, M. W., Moss, D. S., and Thornton, J. M. (1993) *J. Appl. Crystallogr. 26*, 283−290.
24. Dworschack, R. T., and Plapp, B. V. (1977) *Biochemistry 16*, 2716−2725.
25. Shearer, G. L., Kim, K., Lee, K. M., Wang, C. K., and Plapp, B. V. (1993) *Biochemistry 32*, 11186−11194.
26. Theorell, H., and Chance, B. (1951) *Acta Chem. Scand. 5*, 1127−1144.
27. Dalziel, K. (1963) *J. Biol. Chem. 238*, 2850−2858.
28. Cleland, W. W. (1963) *Biochim. Biophys. Acta 67*, 173−187.
29. Cleland, W. W. (1963) *Biochim. Biophys. Acta 67*, 188−196.
30. Ramaswamy, S., Scholze, M., and Plapp, B. V. (1997) *Biochemistry 36*, 3522−3527.
31. Ramaswamy, S., Eklund, H., and Plapp, B. V. (1994) *Biochemistry 33*, 5230−5237.
32. Fan, F., and Plapp, B. V. (1995) *Biochemistry 34*, 4709−4713.
33. Northrop, D. B. (1982) *Methods Enzymol. 87*, 607−625.
34. Gould, R. M., and Plapp, B. V. (1990) *Biochemistry 29*, 5463−5468.
35. Kvassman, J., and Pettersson, G. (1978) *Eur. J. Biochem. 87*, 417−427.
36. Schowen, K. B., and Schowen, R. L. (1982) *Methods Enzymol. 87*, 551−606.
37. Eklund, H., Nordström, B., Zeppezauer, E., Söderlund, G., Ohlsson, I., Boiwe, T., Söderberg, B.-O., Tapia, O., Brändén, C.-I., and Åkeson, Å. (1976) *J. Mol. Biol. 102*, 27−59.
38. Eklund, H., Samama, J.-P., Wallén, L., Brändén, C.-I., Åkeson, Å., and Jones, T. A. (1981) *J. Mol. Biol. 146*, 561−587.
39. Plapp, B. V., Eklund, H., and Brändén, C.-I. (1978) *J. Mol. Biol. 122*, 23−32.
40. Brändén, C.-I., and Eklund, H. (1978) *Ciba Found. Symp. 60*, 63−80.
41. Li, H., Hallows, W. H., Punzi, J. S., Marquez, V. E., Carrell, H. L., Pankiewicz, K. W., Watanabe, K. A., and Goldstein, B. M. (1994) *Biochemistry 33*, 23−32.
42. Cedergren-Zeppezauer, E. S., Andersson, I., Ottonello, S., and Bignetti, E. (1985) *Biochemistry 24*, 4000−4010.
43. Plapp, B. V., Eklund, H., Jones, T. A., and Brändén, C.-I. (1983) *J. Biol. Chem. 258*, 5537−5547.
44. Sun, H.-W., and Plapp, B. V. (1992) *J. Mol. Evol. 34*, 522−535.
45. Mewes, H. W., Albermann, K., Heumann, K., Liebl, S., and Pfeiffer, F. (1997) *Nucleic Acids Res. 25*, 28−30.
46. Korkhin, Y., Kalb(Gilboa), A. J., Peretz, M., Bogin, O., Burstein, Y., and Frolow, F. (1998) *J. Mol. Biol. 278*, 967−981.
47. Ramaswamy, S., El Ahmad, M., Danielsson, O., Jörnvall, H., and Eklund, H. (1994) *Protein Sci. 5*, 663−671.
48. Pettersson, G. (1987) *CRC Crit. Rev. Biochem. 21*, 349−389.
49. Belasco, J. G., Albery, W. J., and Knowles, J. R. (1983) *J. Am. Chem. Soc. 105*, 2475−2477.
50. Quinn, D. M., and Sutton, L. D. (1991) in *Enzyme Mechanism from Isotope Effects* (Cook, P. F., Ed.) pp 73−126, CRC Press, Boca Raton, FL.
51. Cleland, W. W., Frey, P. A., and Gerlt, J. A. (1998) *J. Biol. Chem. 273*, 25529−25532.
52. Hu, W.-P., and Truhlar, D. B. (1994) *J. Am. Chem. Soc. 116*, 7797−7800.
53. LeBrun, L. A., and Plapp, B. V. (1999) *Biochemistry 38*, 12387−12393.

BI991731I